

Synthesis and Characterization of Constrained Peptidomimetic Dipeptidyl Peptidase IV Inhibitors: Amino-Lactam boroAlanines

Jack H. Lai, Wengen Wu, Yuhong Zhou, Hlaing H. Maw, Yuxin Liu, Lawrence J. Milo, Jr., Sarah E. Poplawski,[†] Gillian D. Henry, James L. Sudmeier, David G. Sanford, and William W. Bachovchin*

Contribution from the Department of Biochemistry, Tufts University School of Medicine, 136 Harrison Avenue, Boston, Massachusetts 02111

Received November 14, 2006

We describe here the epimerization-free synthesis and characterization of a new class of conformationally constrained lactam aminoboronic acid inhibitors of dipeptidyl peptidase IV (DPP IV; E.C. 3.4.14.5). These compounds have the advantage that they cannot undergo the pH-dependent cyclization prevalent in most dipeptidyl boronic acids that attenuates their potency at physiological pH. For example, D-3-amino-1-[L-1-boronic-ethyl]-pyrrolidine-2-one (amino-D-lactam-L-boroAla), one of the best lactam inhibitors of DPP IV, is several orders of magnitude less potent than L-Ala-L-boroPro, as measured by K_i values (2.3 nM vs 30 pM, respectively). At physiological pH, however, it is actually more potent than L-Ala-L-boroPro, as measured by IC_{50} values (4.2 nM vs 1400 nM), owing to the absence of the potency-attenuating cyclization. In an interesting and at first sight surprising reversal of the relationship between stereochemistry and potency observed with the conformationally unrestrained Xaa-boroPro class of inhibitors, the L-L diastereomers of the lactams are orders of magnitude less effective than the D-L lactams. However, this interesting reversal and the unexpected potency of the D-L lactams as DPP IV inhibitors can be understood in structural terms, which is explained and discussed here.

Introduction

Dipeptidyl peptidase IV (DPP IV; E.C. 3.4.14.5) is a serine protease found on the surface of nearly every organ and tissue in the body.¹ It is strongly expressed on the surface of T cells, where it is also known as CD26, a T cell activation antigen.² But it also occurs in soluble form in plasma and other body fluids.³ As an enzyme, DPP IV cleaves dipeptides from the amino terminus of peptides and proteins containing either L-proline or L-alanine at the penultimate position.⁴ Such removal of a dipeptide from the N-terminus of the incretin hormones glucagon-like peptide-1 (GLP-1) and glucose-dependent insulinotropic peptide (GIP) eliminates their biological activities.⁵ Because GLP-1 and GIP have multiple activities, all of which would be highly desirable attributes in an antidiabetogenic drug, and because DPP IV has been shown to be largely responsible for the very short half-life of these hormones in vivo,⁶ inhibitors of DPP IV are of substantial interest for their therapeutic potential in the treatment of type II diabetes.⁷

Dipeptide proline boronic acids of the type Xaa-boroPro (boroPro refers to proline in which the C-terminal carboxylate has been replaced by a boronyl group and Xaa is any unblocked amino acid) are among the most potent inhibitors of DPP IV known.^{8–10} For example, L-Pro-L-boroPro has a K_i value of 16 pM for DPP IV.⁹ However, these inhibitors undergo a reversible, pH-dependent intramolecular cyclization between the N-terminal amine and the C-terminal boron (Figure 1).^{11,12} The cyclic structure, favored at high pH, is devoid of inhibitory activity. Thus, the net effect of the pH-dependent cyclization reaction is to attenuate the potency of these inhibitors at

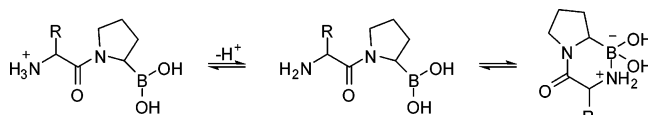


Figure 1. pH-Dependent equilibrium between linear and cyclic forms of Xaa-boroPro. The open chain form (left) is favored at low pH values, and the cyclic form (right) is favored at high pH.

physiological pH. The attenuation can be quite large. For L-Ala-L-boroPro, for example, it is several 1000-fold.¹³

Cyclization can be eliminated by N-terminal substitutions that render the unshared electron pair on the N-terminal nitrogen unavailable for nucleophilic attack on the boron, such as acylation or trimethylation. However, such substituents also strongly reduce inhibitor potency toward DPP IV^{8,14} because they render the electron pair unavailable for protonation, and a protonated amino group is required for binding of both substrates and inhibitors. N-Alkylations that leave the unshared pair available for protonation can reduce the tendency to cyclize, largely through steric hindrance, but also often reduce inhibitory potency as well.¹⁵

In an effort to prevent the intramolecular N–B cyclization, while retaining an unsubstituted N-terminal amino group, we synthesized two stereospecifically constrained peptidomimetics amino-D-lactam-L-boroAla (**1**) and amino-L-lactam-L-boroAla (**2**), as boronic acid analogs to Freidinger's five-membered lactam-bridged dipeptide scaffold.¹⁶

As depicted in Figure 2, these lactam analogs are derived from the previously reported DPP IV inhibitor L-Ala-L-boroPro (**3**)¹³ and its epimer D-Ala-L-boroPro (**4**). Most notably, the cyclic pyrrolidine moiety at P1 is replaced by an acyclic amino acid (alanine) analog. In these lactam analogs, by breaking apart atoms C5 and C6 and connecting C4 and C5, ω is locked into the *trans* conformation ($\sim 180^\circ$), the conformation that binds to the enzyme. Furthermore, the angle ψ becomes part of the five-membered lactam ring, and inspection of the molecular models reveals that it is restricted to $120 \pm 30^\circ$ in compound **1**

* To whom correspondence should be addressed. Phone: 617-636-6881. Fax: 617-636-2409. E-mail: william.bachovchin@tufts.edu.

[†] Present address: Department of Neurology, Brigham and Women's Hospital, 75 Francis Street, Boston, Massachusetts 02115.

^a Abbreviations: HSQC, heteronuclear single quantum coherence; NOESY, nuclear Overhauser spectroscopy; K_i , inhibition constant; IC_{50} , median inhibition concentration.

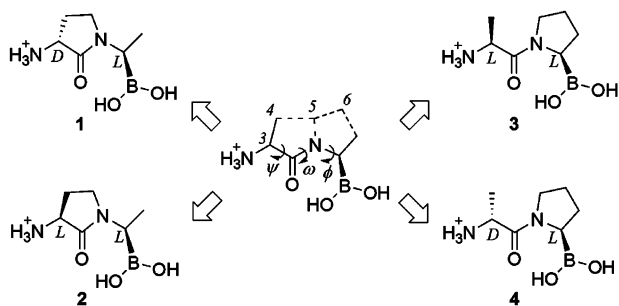


Figure 2. Design of the γ -lactam boronate derivatives. The cyclic pyrrolidine moiety in **3** and **4** is replaced by the corresponding acyclic amino acid **1** and **2**.

and $-120 \pm 30^\circ$ in **2** (the flexibility of $\pm 30^\circ$ or somewhat more is due to the puckering of five-membered rings).

We report here the success of this backbone-constraining strategy in the epimerization-free synthesis and characterization of a noncyclizing boronic acid DPP IV inhibitor of low nanomolar potency. The paradoxical identity of the active epimer has led to increased insight for the design of DPP IV inhibitors.

Results and Discussion

Chemistry. Table 1 summarizes the compounds synthesized in this study. Compounds **3–6** were resynthesized, following the procedures previously reported by the authors.¹³

The key to the synthesis of the target amino- γ -lactam boronates (**1,2**) involves use of an appropriate leaving group to aid intramolecular nitrogen-carbon bond formation upon treatment with a strong base. We investigated various synthetic routes starting from protected chiral dipeptides for the synthesis of each γ -lactam derivative, however, several resulted in epimerization at the P2 α -carbon.

A Boc-protected dipeptide derivative containing a side chain sulfonium salt¹⁶ was used in the synthesis of **1** and **2**. This enabled lactam ring formation through intramolecular alkylation of the amide nitrogen. As shown in Scheme 1 (route A), commercially available *N*-Boc-*L*-methionine (**7**) was first condensed with *L*-boroAla-pn hydrochloride¹⁸ under standard coupling conditions¹⁹ to afford the protected methionine dipeptide (**8**) in 88% yield. Treatment of **8** with methyl iodide followed by sodium hydride in 1:1 DMF/DCM gave crude protected dipeptide lactam. Without further purification of the crude mixture, concurrent removal of the Boc and pinane groups by BCl_3 gave a 1:19 diastereomeric ratio of **1** and **2**, as revealed by ^1H NMR analysis, in 41% yield. Presumably, the minor product (**1**) resulted from the epimerization of the P2 α -proton by use of the strong base used in the lactam ring formation step. Replacement of sodium hydride with either a stoichiometric or a smaller amount of the *N*-methylacetamide lithium salt²⁰ did not reduce the amount of **1** formed. Although **1** and **2** are both desired targets of this study, it was difficult to separate them via HPLC due to their similar retention times and high polarities. Attempts to purify the corresponding protected precursors by HPLC or silica gel chromatography also failed.

To reduce the amount of epimerization resulting from the intramolecular alkylation reaction in the synthesis of **2**, a different leaving group was sought (route B of Scheme 1). The hydroxyl group of the P2 side chain was converted to the mesylated alcohol to aid in the intramolecular nitrogen-carbon bond formation. Following a standard peptide synthesis protocol, commercially available *N*-Boc-*O*-benzyl-*L*-homoserine (**9**) was coupled to *L*-boroAla-pn using HATU. Compound **10** was obtained in 53% yield upon deprotection of the *O*-benzyl group

via palladium-catalyzed hydrogenation. The hydroxyl group of **10** was mesylated by MsCl and cyclized with the amide nitrogen, followed by treatment with 1 equiv of LDA to form the pyrrolidinone boronic ester.²¹ Following the workup, the crude product was deprotected using BCl_3 , which gave a mixture of the HCl salts of pyrrolidinoneboronic acids **1** and **2**. The combined yield of the final three synthetic steps was 46%, with the ratio of **1:2** ranging from 1:4 to 1:19.

Compound **1** was first prepared from the commercially available *N*-Boc-*D*-methionine (**11**), following the strategy depicted in Scheme 2. However, the ratio of diastereomers **1** to **2** was 1.5:1, as determined by ^1H NMR. In addition, the cyclopropyl-bearing byproduct (**12**), resulting from the intramolecular C-alkylations of the corresponding methionine sulfonium salts, was also isolated. The ratio of these isolates (**1:2:12**) was 9:6:5.

To enhance the stereopurity of **1**, we used the unique properties of the 9-phenylfluorenyl (Pf) protecting group.²² The steric bulk of the Pf group attached to the amine of an optically pure methionine prevents deprotonation at $\text{C}\alpha$ by strong bases and results in proton abstraction exclusively at the amide nitrogen. Introduction of the Pf group involved conversion from the pre-existing Boc group. This was accomplished by treating **13** with 4 *N* HCl in dioxane, followed by protection, using *N*-Pf formation conditions²³ to afford *N*(Pf)-Met-boroAla-pn (**14**) in a yield of 79% (Scheme 3). Compound **14** was subsequently converted to the sulfonium salt by reaction with methyl iodide. Formation of the lactam ring was induced by sodium hydride in 1:1 DMF/methylene chloride. Deprotection of the crude dipeptide derivative by BCl_3 , followed by HPLC purification, gave the desired pyrrolidinoneboronic acid (**1**) as a hydrogen chloride salt (24% overall yield in three steps). The final product was verified by ^1H NMR, which indicated that epimerization was successfully avoided. The same method was used to give the pure *L*-diastereoisomer (**2**; 16% total yield in five steps), starting with *L*-*N*-Boc-Met-*L*-BoroAla-pn (**8**; Scheme 3).

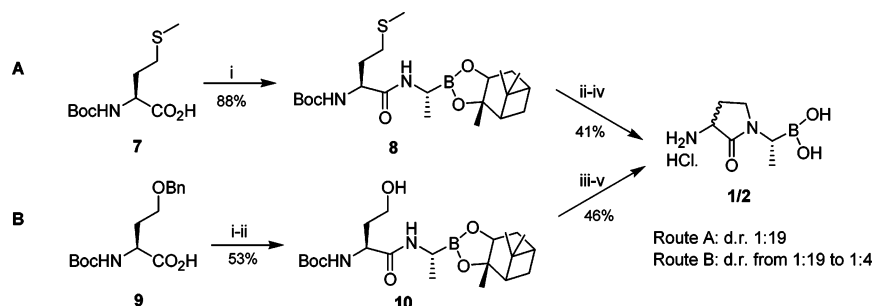
Finally, formation of an undesired structural isomer, azetidines (**15**), via terminal *N*-alkylation (path B, Scheme 4) instead of the desired lactam (**2**), via amide *N*-alkylation (path A, Scheme 4), was a concern throughout the synthesis of the target lactam derivative (**2**; the same concern was applied to **1**). To confirm this, we synthesized **15** via a three-step synthetic procedure starting with *L*-azetidines-2-carboxylic and showed that it has different characteristics than **2** in HPLC retention time and ^1H 1D and 2D NOESY NMR spectra. Confirming evidence arises from the biological assay with DPP IV: compound **2** is about 7-fold less potent than **15** and exhibits a pH-independent inhibition profile, in contrast to the pH-dependent profile of **15**.

Enzyme Assay. Our previous studies of Xaa-boroPro dipeptides showed that DPP IV inhibitors exist predominantly in the open, *trans* form of proline at low pH values (e.g., **2**) and in the cyclic, *cis* form at high pH (e.g., **8**).^{11,12} Half-lives for cyclization and uncyclization of these boroPro inhibitors are typically measured in hours,¹² largely due to the high-energy barrier of proline *cis-trans* interconversion. Because assays can be performed in a matter of minutes, and the cyclic structures are noninhibitory, the ratio of the cyclic (inactive) to open chain (active) material can be easily approximated using simple enzyme inhibition assays. The inhibitor is incubated in solution of a given pH (typically pH 8.0 and 2.0), long enough (generally 24 h) to allow the open and cyclic structures to reach equilibrium. The inhibitors are then added to an assay solution at pH 8.0 containing enzyme, and incubated for 10 min before substrate is added and the enzyme activity is measured. Ten

Table 1. Summary of Boronic Acids Synthesized, Torsional Angles Calculated by Ab Initio Methods, and Their Inhibition Parameters vs DPP IV

compd	name ^a	ψ (P2) (deg)	ω (deg)	ϕ (P1) (deg)	K_i (nM)	IC ₅₀ ^b (pH 2, nM)	IC ₅₀ ^b (pH 8, nM)	CI ^c
1 ^d	amino-D-lactam-L-boroAla	+146.3	+163.9	-86.5	2.3 ± 0.4	5.3 ± 0.3	4.2 ± 0.2	0.8
2 ^d	amino-L-lactam-L-boroAla	-106.5	+153.9	-73.5	1100 ± 110	480 ± 50	460 ± 30	1.0
3 ^e	L-Ala-L-boroPro	+155.4	+171.5	-64.4	0.03 ± 0.01	0.54 ± 0.08	1,400 ± 200	2600
4 ^e	D-Ala-L-boroPro	-158.0	+177.8	-62.5		21 000 ± 3000 ^f	≥21 000 ^f	
5 ^e	L-Val-L-boroPro	+156.6	+173.5	-65.2	0.18 ± 0.03	1.6 ± 0.3	1200 ± 100	750
6 ^e	D-Val-L-boroPro	-160.2	+176.5	-60.5		2300 ± 200 ^f	≥2300 ^f	

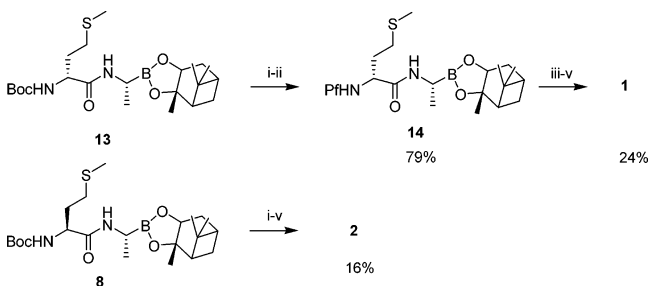
^a We have avoided the (*S*) and (*R*) absolute configuration nomenclature here because of the confusing quirk that substitution of the -B(OH)₂ group for -CO₂H in boronic acids results in a switch from the (*S*) to the (*R*) configuration and vice versa because of the Cahn-Ingold-Prelog priority rules.¹⁷ For example, (*S*)-Ala-(*S*)-Pro is the stereochemical homolog of L-Ala-L-Pro, and (*S*)-Ala-(*R*)-boroPro is the stereochemical homolog of L-Ala-L-boroPro. ^b IC₅₀ values obtained for the inhibitors equilibrated at pH 2 and pH 8 for times ranging from 18 to 24 h prior to addition to the enzyme. ^c Cyclization index, ratio of IC₅₀ values at pH 8 over those at pH 2. ^d Angles computed by HF/6-31G* method, with subsequent MP2/6-31G* refinement. ^e Angles computed by HF/6-31G* method. ^f Inhibition most likely due to the presence of a minute amount of the active diastereomer.⁹

Scheme 1. Routes for the Preparation of **2** from *N*-Boc-L-Methionine (**7**)^a and *N*-Boc-L-Homoserine (OBn; **9**)^b

^a Reagents and conditions (route A): (i) L-boroAla-pn·HCl salt, HATU, DIPEA, DMF; (ii) MeI; (iii) NaH, DMF, DCM, 0 °C; (iv) BCl₃, DCM. ^b Reagents and conditions (route B): (i) L-boroAla-pn·HCl salt, HATU, DIPEA, DMF; (ii) H₂, Pd-C, EtOAc; (iii) MsCl, NEt₃, DCM; (iv) LDA, THF, -78 °C; (v) BCl₃, DCM.

Scheme 2. Preparation of **1** from *N*-Boc-D-Methionine (**11**)^a

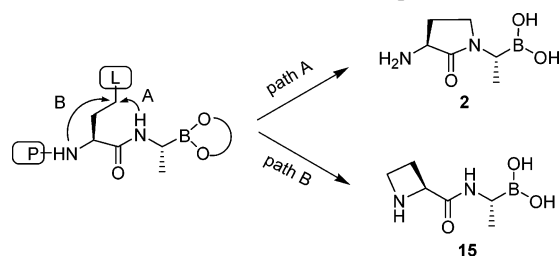
^a Reagents and conditions: (i) L-boroAla-pn·HCl, HATU, DIPEA, DMF; (ii) MeI; (iii) NaH, DMF, DCM, 0 °C; (iv) BCl₃, DCM. Combined yield: 32% (**1**:**2** = 9:6:5).

Scheme 3. Synthesis of **1** and **2** Using Pf as N Protection Group^a

^a Reagents and conditions: (i) HCl, dioxane; (ii) PfBr, NEt₃, Pb(NO₃)₂, K₃PO₄, MeCN; (iii) MeI; (iv) NaH, DMF, DCM, 0 °C; (v) BCl₃, DCM.

minutes was found optimal to give the slow-binding inhibitors enough time to complex, yet not enough time to appreciably shift the *cis*-*trans* equilibrium. The cyclization index (CI), calculated by dividing the IC₅₀ obtained at high pH by that at low pH (IC₅₀ (pH 8)/IC₅₀ (pH 2)), was used as a means of evaluating the cyclization tendency for each compound at physiological pH. The greater the value of CI, the more the equilibrium favors the cyclization.

In this paper, we report both IC₅₀ and K_i values for each inhibitor. The IC₅₀ is the molar concentration of the inhibitor that produces 50% inhibition of the enzyme activity. K_i , the

Scheme 4. Possible Reaction Paths to Compounds **2** and **15**^a

^a Path A: amide *N*-alkylation. Path B: terminal *N*-alkylation. L = leaving group; P = protective group.

inhibition constant, is a measure of the enzyme-inhibitor binding strength. It is much more difficult to measure than IC₅₀, owing to the slow, tight binding characteristics and the cyclization reaction of these inhibitors. We have previously pointed out these difficulties and have developed new methods for solving the problems.⁹ For these inhibitors, IC₅₀ is valuable for two reasons. First it provides a convenient way to measure their cyclization tendency. Second, and perhaps more importantly, the IC₅₀ value is a better predictor of inhibitor effectiveness at physiological pH.

Inhibition of DPP IV by compounds **1**-**6** was evaluated and the results summarized in Table 1. Results indicate that L-Ala-L-boroPro (**3**) and L-Val-L-boroPro (**5**) are among the most potent inhibitors of DPP IV, with subnanomolar K_i values. The corresponding lactam, amino-L-lactam-L-boroAla (**2**), is less potent by 3 to 4 orders of magnitude. Interestingly, however, the opposite diastereomeric homolog, amino-D-lactam-L-boroAla (**1**), inhibits some 500 times better, with a K_i value of 2.3 nM. The CI values of compounds **3** and **5** are 2600 and 750, respectively. In contrast, the IC₅₀ values for the lactams **1** and **2** are pH-independent (CI ~ 1), confirming that they do not cyclize.

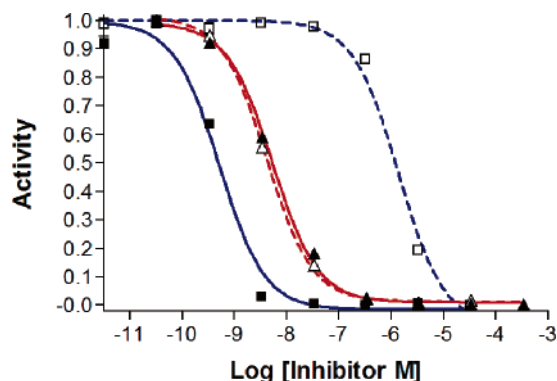


Figure 3. pH Dependence of lactam (**1**) vs L-Ala-L-boroPro (**3**): unconstrained boronate L-Ala-L-boroPro (**3**, blue lines, squares) and constrained lactam derivative amino-D-lactam-L-boroAla (**1**, red lines, triangles). Solid lines and filled symbols are at pH 2.0; dashed lines and open symbols are at pH 8.0.

Figure 3 compares enzyme inhibition curves of **1** and **3** as a function of pH. It shows, as expected, that the inhibitory potency of **3** is markedly pH dependent; the IC₅₀ varies about 2,300-fold, depending on whether **3** has been equilibrated at pH 2.0 or pH 8.0. The loss of inhibitory potency of **3** on equilibrating at pH 8.0 is not irreversible, and can be fully recovered via 24 h in solution at pH 2.0. Compound **5** exhibits a similar, though somewhat smaller, pH dependence with a CI of ~750 (not shown in Figure 3). In contrast, the inhibitory potency of lactams **1** (shown in Figure 3) and **2** (not shown) are entirely pH-independent, thereby confirming our original expectation that restrained structures would not cyclize. Note, while Figure 3 shows that **1** is clearly not as potent as **3** when **3** has been equilibrated at pH 2.0, it also shows that **1** is actually more potent than **3** at high pH values and, therefore, suggests that **1** could be more potent than **3** in vivo.

The inhibitory activity of lactam **2** could have been caused by a trace amount (ca. <1%) of **1** in the **2** sample; however, none was detected by ¹H NMR or LC-MS.

Computational Analysis. Molecular modeling was employed to help ascertain from theory the conformational forms adopted by compounds **1–6** (Table 1). Although psi and omega in compounds **1** and **2** and phi in **3–6** are known approximately from their ring constraints, for consistency all calculated values of psi, omega, and phi are listed in Table 1. Gas-phase calculations of the conformations of small molecule inhibitors in solution have obvious limitations, but our sole aim here is to seek any correlation of backbone conformation with IC₅₀ values for drug design purposes.

The six DPP IV inhibitors discussed here exhibit various degrees of backbone conformational flexibility. For all compounds, the calculated omega (ω) angles were not far from 180°, producing a *trans*, planar amide bond relative to the opposing α -carbons. In the lactams **1** and **2**, omega is constrained by inclusion in the closed rings to the *trans* conformer. Psi values vary widely from about +150° for **3** and **5**, to -160.5° for **2**, to about -160° in **4** and **6**. From Table 1 it is clear that all the highly effective inhibitors have psi angles in the +150° neighborhood, regardless of the stereochemical configuration about the P2 alpha carbon. This psi angle is similar to those found for bound inhibitors in x-ray crystallographic studies,^{24–26} as shown in Table 2.

In the bound state, a *trans* (~180°) torsion angle omega, or ω ($C_{\alpha}-C-N-C_{\alpha}$), is required. Table 2 also shows the values of psi, or ψ ($N-C_{\alpha}-C-N$), and phi, or ϕ ($C-N-C_{\alpha}-C$), determined by X-ray crystallography of bound ligands.

Table 2. Summary of Backbone Angles of Inhibitors Bound to DPP IV by X-ray Crystallographic Determination of Structures of Complexes. Multiple Entries Are Due to the Presence of Two or Four Liganded Proteins Per Unit Cell.

ID ²⁴	inhibitor ^a	ψ (P2) (deg)	ω (deg)	ϕ (P1) (deg)	res.	ref.
1WCY	L-Ile-L-Pro-L-Ile	133.9	179.6	-78.1	2.20 Å	25
		129.4	179.7	-76.1		
2AJB	L- <i>t</i> -BuGly-L-Pro-L-Ile	134.7	-179.9	-80.0	2.75 Å	26
		133.0	-179.9	-84.5		
		133.4	-179.9	-83.9		
		127.7	180.0	-86.3		
2AJD	L-Pro-L-boroPro	160.4	-179.9	-86.1	2.56 Å	26
		169.9	179.8	-74.5		
		162.2	179.8	-78.6		
		154.4	180.0	-87.6		

^a We have avoided the (*S*) and (*R*) absolute configuration nomenclature here because of the confusing quirk that substitution of the -B(OH)₂ group for -CO₂H in boronic acids results in a switch from the (*S*) to the (*R*) configuration and vice versa because of the Cahn-Ingold-Prelog priority rules.¹⁷ For example, (*S*)-Pro-(*S*)-Pro is the stereochemical homolog of L-Pro-L-Pro, and (*S*)-Pro-(*R*)-boroPro is the stereochemical homolog of L-Pro-L-boroPro.

The calculated phi angles in Table 1 vary from -60.5° to -86.5°. For comparison, the phi values of bound inhibitors in Table 2 vary from -74.5° to -86.3°. Interestingly, of the compounds listed in Table 1, phi of lactam **1** seems to be the most optimally set for enzyme binding, which probably helps to explain the potency of this constrained derivative. The other inhibitors in Table 1 (**3–6**) have phi values of ~-60°, which is ~15° to 20° away from optimal for enzyme binding. Note that **3** and **5** are extremely potent enzyme inhibitors, while **4** and **6** are devoid of inhibitory potency, yet all have essentially the same phi value. These differences are obviously determined by the stereochemical configuration about P2. Thus, significance of phi values for inhibitory potency cannot be assessed from the current data.

What are the important contacts in the bound state of good DPP IV inhibitors? As detailed in the X-ray crystallographic studies of bound inhibitors,^{25,26} there are as many as three H-bonds to the protonated N-terminal amino group of the P2 residue arising from Glu205, Glu206, and Tyr662. The carbonyl oxygen of P2 is H-bonded to the carboxamide group of Asn710 and guanidyl of Arg125. The P1 pyrrolidine ring packs into the S1 groove, attracted by hydrophobic forces. Only the L-L diastereomer of the L-Pro-L,D-boroPro racemate binds to DPP IV,²⁶ showing the stereospecific contacts involving the N-terminal nitrogen, the boron atom, and the pyrrolidine ring. The boron adduct to Ser630 is tetrahedral, with one of its hydroxyl groups bound to the oxyanion hole (from Tyr547 and Ser631) and the other bound to the catalytic His740.

Figure 4 shows our hypothetical scheme for rationalizing X-ray data and inhibitor binding, showing the inhibitors from their N-terminus along the C α -C=O bond of residue P2. The dihedral angle between successive nitrogen atoms is the backbone angle psi, whose approximate value is shown in each subfigure. Figure 4a represents a composite of the X-ray structures in Table 2, with five of the important H-bonds from the enzyme to the ligand. Although there are no X-ray structures of compounds **3** or **5**, we expect that their backbones would superimpose nicely on these structures, as shown in Figure 4a. No X-ray structures exist yet for compounds **1**, **2**, **4**, or **6** either, but we can infer how H-bonding and steric repulsion might influence the fit of these compounds and, thus, inhibitory potency in the active site through the use of Figure 4b-d.

Figure 4a shows H-bonds donated from the enzyme to inhibitors with P2 in the L configuration, which in solution are

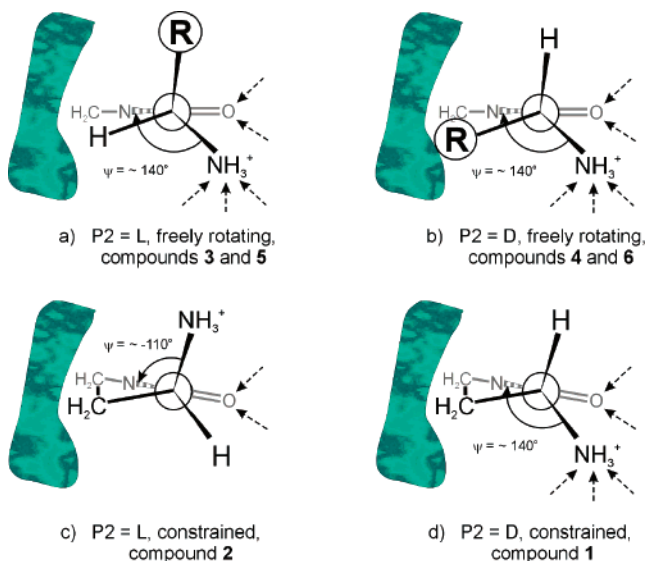


Figure 4. Schematic of proposed conformations of residue P2 for unconstrained and lactam-constrained inhibitors bound to DPP IV active site. The barrier or “wall” is comprised of the aromatic side chains of Tyr666 and Phe357, as shown in X-ray structures.²⁶

free to rotate about psi, namely, **3** and **5**. A nominal psi value of $\sim 140^\circ$ is adopted, which is close to the average of the inhibitor angles found in X-ray structures (Table 2). The C=O—NH group lies behind in the horizontal plane, roughly the plane of the pyrrolidine ring. The “wall” is formed by aromatic side chains of Tyr666 and, perhaps to a lesser extent, Phe357.

There is plenty of room for the R groups in **3** and **5** (methyl and *i*-propyl) in Figure 4a, accounting for their favorable binding in Table 1. In addition, we have the fact that the *t*-Bu group in X-ray structure 2AJB is easily accommodated, and in L-Pro-L-boroPro (2AJD) the entire P2 proline ring lies in the region shown by the R group, more or less perpendicular to the P1 proline ring. Figure 4b shows the steric repulsion between the enzyme “wall” and the side chain R, which would exist in the bound state for the D configuration of P2 when all other contacts to the enzyme are formed. This argument can explain broadly why **4** and **6** are such poor inhibitors.

Compound **2** is shown in Figure 4c as it might fit into the active site with its boronate and carbonyl H-bonds to the enzyme intact. Clearly, because of the lactam ring constraint, **2** cannot form the N-terminal H bonds and, even with its otherwise favorable L configuration, forms a poor inhibitor. Compound **1**, depicted in Figure 4d can form all the correct H-bonds to DPP IV, despite its unfavorable D configuration. The difference in IC₅₀ values between **1** and **3** could well be explained by some steric repulsion to the lactam ring —CH₂— group occurring in **1**, as depicted in 4d. However, lactams **1** and **2**, having no pyrrolidine ring, need not fit in the active site exactly the same as compounds **3**–**6**. This is suggested in Figure 4c,d by a slight rotation of the lactams in such a way as to relieve steric repulsion. Such a difference in binding could provide the needed explanation for why lactam **1** is so much better an inhibitor than **4** and **6**, all possessing the D configuration.

The differences in IC₅₀ values of **1** vs **4** and **6** must also arise from the entropic advantage of the former. A flexible inhibitor arriving at the active site preformed to the bound state conformation will enjoy an entropic advantage due to higher effective concentration and thus reflected in a higher “on rate”.²⁷ As shown in Table 1, the theoretical values of psi have the opposite sign ($\sim -160^\circ$) for **4** and **6** in free solution instead of the $\sim +140^\circ$ presumably required for binding. The relevant

k_{on} and k_{off} rates should demonstrate that lactam **1** binds far better than **4** and **6** because of its preformed psi as well as omega angles as a result of the lactam ring constraints.

Conclusions

Conformationally restricted dipeptide boronates containing a five-membered lactam ring (amino-lactam-L-boroAla) are synthesized with L- and D-epimers. Among them, the D-epimer (**1**) is found to be a very potent DPP IV inhibitor, exhibiting a K_i value of 2.3 nM, whereas the L-epimer (**2**) showed only moderate potency. The backbone constraint imposed by the lactam peptidomimetic eliminates the N—B cyclization observed in most dipeptide boronic acids. The biological activities of the epimers are correlated with the greater similarity to the backbone conformation of bound inhibitors, as revealed by X-ray crystallographic studies of DPP IV complexes. The increased stability should make these compounds effective at lower doses in animal studies, with a longer duration of action. To our knowledge, this is the first time that backbone-constrained peptidomimetic inhibitors with low nanomolar potency for DPP IV have been reported.

Experimental Section

Materials and Analysis. Reagents obtained from commercial sources were used without further purification. NMR spectra were recorded on a Bruker Avance 300 MHz spectrometer. Chemical shifts were reported in parts per million (δ scale) relative to TMS (in CDCl₃) or DSS (in D₂O) for ¹H and ¹³C NMR and boric acid (in D₂O) for ¹¹B NMR. Mass spectra and HPLC retention times were recorded on a Hewlett Packard HP LC/MSD system with UV detector (monitoring at 215 nm), using a Discovery C18 569232-U RP-HPLC column (12.5 cm \times 4.6 mm, 5 μ m) with solvent gradient A = water (0.1% TFA) and B = acetonitrile (0.08% TFA) at 0.5 mL/min. Unless otherwise noted, all HPLC retention times are given for an eluent gradient 2% B for the first 5 min, then from 2% to 98% B over 10 min, which was maintained for the next 10 min. The crude targets were purified by RP-HPLC using a Varian semipreparative system with a Discovery C18 569226-U RP-HPLC column (25 cm \times 21.2 mm, 5 μ m) at 20 mL/min. HRMS were performed by the Technical Services of the University of Michigan.

DPP IV Inhibition Assay. Dipeptidyl peptidase IV was purified from human placenta.²⁸ Assays were performed at ambient temperature (23 $^\circ$ C) in 100 mM HEPES, pH 8.0, 0.14 M NaCl, with the chromogenic substrate Ala-Pro-*p*-nitroanilide (Bachem). Approximately 1 nM of DPP IV enzyme was incubated with various inhibitor concentrations, ranging between 10^{-4} and 10^{-11} M, for 10 min before starting the reaction by the addition of substrate to a concentration of 30 μ M. The absorbance at 410 nm was measured 30 min after the addition of substrate. The IC₅₀ value is defined as the concentration of inhibitor required to reduce the DPP IV activity to 50% after a 10-minute incubation with the enzyme at 23 $^\circ$ C and before the addition of the substrate. IC₅₀ values were determined by a nonlinear regression fit of the data to a sigmoidal dose–response curve using the program Prism. DPP IV inhibition assays were performed at 25 $^\circ$ C on a Molecular Devices SPECTRAMax 340PC³⁸⁴ microtiter plate reader, monitoring the absorbance at 410 nm and using H-AlaPro-pNA (Bachem) as a chromogenic substrate. Inhibitor stock solutions (ca. 1 mg/mL) were prepared in either 0.01 N HCl solution, pH 2.0, or 0.1 M HEPES, 0.14 M NaCl buffer, pH 8.0. All Xaa-boroPro inhibitors were allowed to stand for at least 18 h to fully establish the *cis*–*trans* equilibrium before assaying. Stock solutions were diluted with respective pH buffers immediately prior to the commencement of the experiment.

Compounds **1** and **2** are reversible competitive inhibitors of DPP IV. K_i values were determined by measuring the reaction rate versus the substrate concentration at three different values of inhibitor concentration. The data were fit by nonlinear regression to the equation

$$v = V_{\max}[S]/\{[S] + K_m(1 + [I]/K_i)\}$$

using the program Prism (GraphPad Software, Inc.). Compounds **3** and **5** are slow, tight binding inhibitors. Measurement of K_i values for these two compounds is further complicated by a slow cyclization reaction that inactivates the inhibitors at the reaction pH. This situation has been specifically addressed for DPP IV inhibitors of this class by Gutheil and Bachovchin.⁹ Following the same procedure, K_i values for compounds **3** and **5** were determined by measuring the reaction rate versus the inhibitor concentration at a fixed substrate concentration equal to 5 times the K_m and the lowest enzyme concentration that allows measurement of the rate in 2 min. The resulting data were fit by nonlinear regression to the simple equilibrium equation, as described by Gutheil and Bachovchin.⁹ The substrate used for all K_i measurements was Ala-Pro-*para*-nitroanilide, which has a K_m value of 15 μ M for DPP IV. Initial rates were determined from a linear fit of the absorbance at 410 nm versus the time over 2 min on a Hewlett Packard 8453 UV/vis spectrophotometer.

Computations. Energy minimizations of these compounds were conducted using BioMedCaChe (version 6.0, Fujitsu, Ltd.) and Spartan (version 04, Wavefunction, Inc., Irvine, CA) programs. First, using the molecular mechanics (MM3) or semiempirical (AM1) method, a systematic search was performed by examining all rotamers. The free-energy minimum structure for each compound was extracted using HF/6-31G* calculations. For compounds **1** and **2**, the structures were further optimized by ab initio calculations at the MP2/6-31G* level. Backbone torsion angles ψ (P2), ω and ϕ (P1) were obtained from the lowest-energy conformer (Table 1).

Circular Dichroism Spectroscopy. Measurements were carried out on a JASCO J-810 CD spectropolarimeter at 25 °C, using a 1 mm quartz cell. Sample concentrations were about 0.25 mg/mL. Samples at pH 8 were in 5 mM phosphate buffer, while pH 2 samples were in 0.01 M HCl.

General Procedure for the Coupling Reaction. To a solution of *N*-(*tert*-butoxycarbonyl)-L-methionine (**7**; 0.50 g, 2.0 mmol) in DMF (8.0 mL) was sequentially added DIPEA (0.75 mL, 4.4 mmol), HATU (0.8 g, 2.2 mmol), and L-boroAla-pn·HCl (550 mg, 2.1 mmol) at 0 °C. The mixture was stirred at room temperature overnight and concentrated in vacuo. The residue was redissolved in EtOAc (50 mL) and washed with 0.1 N KHSO₄ (3 × 15 mL), saturated aq NaHCO₃ (2 × 15 mL), and brine. The organic layer was then dried with MgSO₄, filtered, and condensed under vacuum.

General Procedure for Pinanediol and Boc Removal. The oily protected crude (1.5 mmol) was dissolved in dry DCM (8.0 mL) and cooled to -78 °C while BCl₃ (1 M in DCM, 8.0 mL) was added dropwise. The mixture was stirred at -78 °C for 1 h and allowed to warm to room temperature for an additional 3–5 min. The reaction mixture was then concentrated in vacuo and redissolved in ether (15 mL). Water (15 mL) was added and the aqueous layer was washed twice with ether (2 × 15 mL). The aqueous layer was concentrated in vacuo and further purified by semipreparative RP-HPLC to afford the target compound as a white powder.

(1R)-1-[(3R)-3-Amino-2-oxopyrrolidin-1-yl]-ethylboronic Acid Hydrochloride (1**).** The target compound was prepared from (**14**) following the same procedure described in Method A. Compound **1** was obtained as a white powder after semipreparative RP-HPLC purification (20% overall yield in three steps). ¹H NMR (D₂O) δ 4.17 (t, $J = 9.5$ Hz, ¹H, H₂NCH), 3.47–3.68 (m, 2H, CONCH₂), 3.13 (q, $J = 7.5$ Hz, ¹H, BCHN), 2.57–2.67 (m, ¹H, H₂NCHCHACHB), 2.04–2.17 (m, ¹H, H₂NCHCHACHB), 1.18 (d, $J = 7.5$ Hz, 3H, BCHCH₃). ¹³C NMR (D₂O) δ 172.30 (CO), 53.42 (H₂NCH), 46.60 (CONCH₂), 41.69 (BCHN), 26.26 (H₂NCHCH₂), 15.16 (BCHCH₃). The ¹H NMR and ¹³C NMR assignments were consistent with the ¹H–¹³C HSQC. ¹¹B NMR (D₂O) δ 10.38 (br s). LC-MS (ESI+) for C₆H₁₃BN₂O₃ m/z (rel intensity): 463.3 ((3 × (M – H₂O) + H)⁺, 3), 309.2 ((2 × (M – H₂O) + H)⁺, 100), 155.3 ((M – H₂O) + H)⁺, 20); tr = 6.0 min (eluent gradient 0.5% B for the first 10 min, then from 0.5% to 20% B over 10 min); purity >99%. HRMS calcd for C₆H₁₃BN₂O₃Na [M + Na]⁺, 195.0917; found, 195.0919.

(1R)-1-[(3S)-3-Amino-2-oxopyrrolidin-1-yl]-ethylboronic Acid Hydrochloride (2**; Method A).** Compound (**8**; 0.68 g, 1.5 mmol) was dissolved in methyl iodide (10 mL) and stirred at room temperature for 3 days. The reaction mixture was concentrated in vacuo and evaporated three times from methylene chloride solution. DMF–DCM (1:1; 16 mL) was added under Ar and cooled to 0 °C. Sodium hydride (0.12 g of a 60% mineral oil suspension, 3 mmol) was added all at once, and the mixture was stirred at 0 °C for an additional 6 h. NH₄Cl (aq, 6.0 mL, half-saturated) was added carefully to quench the reaction. The solution was concentrated in vacuo to a small volume and partitioned between water (10 mL) and EtOAc (20 mL). The aqueous phase was extracted with EtOAc (2 × 20 mL). The combined organic phase was washed with aq NaHCO₃ and brine and then dried with MgSO₄. After filtration and concentration in vacuo, a pale yellow oil was yielded. Following the general procedure for pinanediol and Boc removal, the target compound (**2**) was obtained as a white powder (0.13 g, 41% yield). ¹H NMR (D₂O) δ 4.18 (t, $J = 9.4$ Hz, ¹H, H₂NCH), 3.47–3.66 (m, 2H, CONCH₂), 3.12 (q, $J = 7.5$ Hz, ¹H, BCHN), 2.57–2.67 (m, ¹H, H₂NCHCHACHB), 2.06–2.16 (m, ¹H, H₂NCHCHACHB), 1.20 (d, $J = 7.5$ Hz, 2.85H, BCHCH₃ of **2**), 1.18 (d, $J = 7.5$ Hz, 0.15H, BCHCH₃ of **1**). LC-MS (ESI+) for C₆H₁₃BN₂O₃ m/z (rel intensity): 463.3 ((3 × (M – H₂O) + H)⁺, 4), 309.2 ((2 × (M – H₂O) + H)⁺, 100), 155.3 ((M – H₂O) + H)⁺, 26); tr = 6.0 min (eluent gradient 0.5% B for the first 10 min and then from 0.5% to 20% B over 10 min); purity (**2** and 5% **1**) > 99%.

(1R)-1-[(3S)-3-Amino-2-oxopyrrolidin-1-yl]-ethylboronic Acid Hydrochloride (2**; Method B).** Methanesulfonyl chloride (0.21 mL, 2.6 mmol) was added dropwise at 0 °C to a DCM solution (20 mL) containing **10** (0.55 g, 1.3 mmol) and NEt₃ (0.72 mL, 5.2 mmol). The ice bath was removed after 30 min, and the mixture was stirred for an additional 4 h at room temperature. A supplementary 20 mL of DCM was added to the mixture, which was then washed with water (10 mL), 0.1 N KHSO₄ (10 mL), saturated aq NaHCO₃ (10 mL), and brine. The organic layer was then dried with MgSO₄, filtered, and concentrated in vacuo. The residue was dissolved in anhydrous THF (10 mL), and LDA (0.6 mL, 2 M, 1.2 mmol) was added dropwise at -78 °C under Ar. The solution was allowed to gradually warm to room temperature and continue to react overnight. The reaction was quenched with saturated aq NH₄Cl (5 mL) and then extracted with EtOAc (2 × 20 mL). The combined organic phase was washed with aq NaHCO₃ and brine and dried with MgSO₄. After filtration and concentration, a pale yellow oil was yielded. Following the general procedure for pinanediol and Boc removal, the target compound was obtained as a white powder (0.13 g, 46% yield). The ¹H NMR spectrum was the same as the one prepared by method A, except the content of **1** was varied from 5% to 20%.

(1R)-1-[(3S)-3-Amino-2-oxopyrrolidin-1-yl]-ethylboronic Acid Hydrochloride (2**; Method C).** Following the same procedure in the preparation of **1**, the target compound was prepared from **8** as a white powder after semipreparative RP-HPLC purification (16% overall yield of the five steps). ¹H NMR (D₂O) δ 4.18 (t, $J = 9.4$ Hz, ¹H, H₂NCH), 3.47–3.66 (m, 2H, CONCH₂), 3.12 (q, $J = 7.5$ Hz, ¹H, BCHN), 2.57–2.68 (m, ¹H, H₂NCHCHACHB), 2.06–2.16 (m, ¹H, H₂NCHCHACHB), 1.20 (d, $J = 7.5$ Hz, 2.85H, BCHCH₃). ¹³C NMR (D₂O) δ 172.29 (CO), 53.48 (H₂NCH), 46.49 (CONCH₂), 41.25 (BCHN), 26.32 (H₂NCHCH₂), 15.31 (BCHCH₃). The ¹H NMR and ¹³C NMR assignments were consistent with the ¹H–¹³C HSQC. ¹¹B NMR (D₂O) δ 10.54 (br s). LC-MS (ESI+) for C₆H₁₃BN₂O₃ m/z (rel intensity): 463.3 ((3 × (M – H₂O) + H)⁺, 6), 309.2 ((2 × (M – H₂O) + H)⁺, 100), 155.3 ((M – H₂O) + H)⁺, 24); tr = 6.0 min (eluent gradient 0.5% B for the first 10 min, then from 0.5% to 20% B over 10 min); purity >99%. HRMS calcd for C₆H₁₃BN₂O₃Na [M + Na]⁺, 195.0917; found, 195.0914.

(1R)-1-[N-(*tert*-Butoxycarbonyl)-L-methionyl]amino-ethylboronate (+)-Pinanediol Ester (8**).** *N*-(*tert*-butoxycarbonyl)-L-methionine (**7**; 0.50 g, 2.0 mmol) was coupled to L-boroAla-pn·HCl (550 mg, 2.1 mmol) following the general procedure for the coupling reaction. The target obtained was a white powder (0.80 g, 88% yield) after flash column chromatography (3/5 EtOAc/

hexanes). ^1H NMR(CDCl_3) δ 6.46 (br s, ^1H , BocNH), 5.24 (br d, ^1H , CHCONH), 4.25–4.31 (m, 2H, BocNHCH, BOCH), 3.20–3.24 (m, ^1H , NHCHB), 2.11–2.56 (m, 4H, SCH_2 , pinane-H), 2.10 (s, 3H, SCH_3), 1.85–2.09 (m, 5H, $\text{CH}_2\text{CH}_2\text{S}$, pinane-H), 1.44 (s, 9H, $(\text{CH}_3)_3\text{C}$), 1.39 (s, 3H, pinane- CH_3), 1.29 (s, 3H, pinane- CH_3), 1.28 (d, $J = 7.7$ Hz, ^1H , pinane-H), 1.22 (d, $J = 7.5$ Hz, 3H, $\text{CH}_3\text{-CHNH}$), 0.84 (s, 3H, pinane- CH_3). LC-MS (ESI+) for $\text{C}_{22}\text{H}_{39}\text{BN}_2\text{O}_5\text{S}$ m/z (rel intensity): 477.3 ($(\text{M} + \text{Na})^+$, 20), 455.3 ($(\text{M} + \text{H})^+$, 89), 399.2 ($(\text{M} - \text{CH}_2 = \text{C}(\text{CH}_3)_2 + \text{H})^+$, 67), 355.2 ($(\text{M} - \text{CH}_2 = \text{C}(\text{CH}_3)_2 - \text{CO}_2 + \text{H})^+$, 20), 303.2 ($(\text{M} - \text{pinane} - \text{H}_2\text{O} + \text{H})^+$, 15), 247.1 ($(\text{M} - \text{CH}_2 = \text{C}(\text{CH}_3)_2 - \text{pinane} - \text{H}_2\text{O} + \text{H})^+$, 100), 203.1 ($(\text{M} - \text{CH}_2 = \text{C}(\text{CH}_3)_2 - \text{CO}_2 - \text{pinane} - \text{H}_2\text{O} + \text{H})^+$, 15); $\text{tr} = 18.3$ min; purity >99%. HRMS calcd for $\text{C}_{22}\text{H}_{40}\text{BN}_2\text{O}_5\text{S}$ [$\text{M} + \text{H}$] $^+$, 455.2751; found, 455.2756.

(1R)-1-[*N*-(*tert*-Butoxycarbonyl)-L-homoseryl]amino-ethylboronate (+)-Pinanediol Ester (10). *N*-(*tert*-Butoxycarbonyl)-O-benzyl-L-homoserine (**9**; 0.62 g, 2 mmol) was coupled to L-boroAla-pn-HCl (550 mg, 2.1 mmol) following the general procedure for coupling reaction except using DCM (15 mL) as solvent. After concentration, the residue was redissolved in EtOAc (15 mL), and 10% Pd/C (100 mg) was added. The mixture was stirred under a hydrogen atmosphere (50 psi) for 5 h. The resulting suspension was filtered through Celite, and the solvent was evaporated. After purification by flash column chromatography using EtOAc/hexanes (4/5), the target was obtained as a white powder (0.45 g, 53% yield). ^1H NMR (CDCl_3) δ 6.57 (br d, ^1H , exchangeable with D_2O , BocNH), 5.57 (br d, ^1H , exchangeable with D_2O , CHCONH), 4.12–4.33 (m, 2H, BocNHCH, BOCH), 3.69–3.73 (m, 2H, CH_2OH), 3.24–3.30 (m, ^1H , NHCHB), 2.85 (br s, ^1H , exchangeable with D_2O , CH_2OH), 1.80–2.35 (m, 7H, $\text{CH}_2\text{CH}_2\text{OH}$, pinane-H), 1.45 (s, 9H, $(\text{CH}_3)_3\text{C}$), 1.41 (s, 3H, pinane- CH_3), 1.29 (s, 3H, pinane- CH_3), 1.23 (d, $J = 7.4$ Hz, 3H, CH_3CHNH), 0.85 (s, 3H, pinane- CH_3). LC-MS (ESI+) for $\text{C}_{21}\text{H}_{37}\text{BN}_2\text{O}_6$ m/z (rel intensity): 447.2 ($(\text{M} + \text{Na})^+$, 11), 425.2 ($(\text{M} + \text{H})^+$, 100), 369.2 ($(\text{M} - \text{CH}_2 = \text{C}(\text{CH}_3)_2 + \text{H})^+$, 69), 325.3 ($(\text{M} - \text{CH}_2 = \text{C}(\text{CH}_3)_2 - \text{CO}_2 + \text{H})^+$, 21), 273.2 ($(\text{M} - \text{pinane} - \text{H}_2\text{O} + \text{H})^+$, 17), 217.2 ($(\text{M} - \text{CH}_2 = \text{C}(\text{CH}_3)_2 - \text{pinane} - \text{H}_2\text{O} + \text{H})^+$, 69), 173.3 ($(\text{M} - \text{CH}_2 = \text{C}(\text{CH}_3)_2 - \text{CO}_2 - \text{pinane} - \text{H}_2\text{O} + \text{H})^+$, 10); $\text{tr} = 15.8$ min; purity >97%.

(1R)-1-(1-Aminocyclopropane-carbonyl)-ethylboronic Acid Hydrochloride (12). The target was prepared from *N*-(*tert*-butoxycarbonyl)-D-methionine (**11**) following the same procedure to prepare (**2**; method A). After semipreparative RP-HPLC purification, the target was afforded as a white powder from (8% overall yield of the four steps). ^1H NMR (D_2O) δ 2.78 (q, $J = 7.4$ Hz, ^1H , BCHN), 1.57–1.59 (m, 4H, cyclopropane-H), 1.09 (d, $J = 7.4$ Hz, 3H, BCHCH $_3$). LC-MS (ESI+) for $\text{C}_6\text{H}_{13}\text{BN}_2\text{O}_3$ m/z (rel intensity): 485.3 ($(3 \times (\text{M} - \text{H}_2\text{O}) + \text{Na})^+$, 3), 463.3 ($(3 \times (\text{M} - \text{H}_2\text{O}) + \text{H})^+$, 31), 309.2 ($(2 \times (\text{M} - \text{H}_2\text{O}) + \text{H})^+$, 100), 155.3 ($(\text{M} - \text{H}_2\text{O} + \text{H})^+$, 31); $\text{tr} = 4.3$ min (eluent gradient 0.5% B for the first 10 min, then from 0.5% to 20% B over 10 min); purity >95%. HRMS calcd for $\text{C}_6\text{H}_{13}\text{BN}_2\text{O}_3\text{Na}$ [$\text{M} + \text{Na}$] $^+$, 195.0917; found, 195.0925.

(1R)-1-[*N*-(*tert*-Butoxycarbonyl)-D-methionyl]amino-ethylboronate (+)-Pinanediol Ester (13). The target compound was prepared from *N*-(*tert*-butoxycarbonyl)-D-methionine (**11**) following the same procedure to prepare (**8**). ^1H NMR (CDCl_3) δ 6.63 (br s, ^1H , BocNH), 5.30 (br d, ^1H , CHCONH), 4.24–4.29 (m, 2H, BocNHCH, BOCH), 3.08–3.12 (m, ^1H , NHCHB), 2.10–2.53 (m, 4H, SCH_2 , pinane-H), 2.07 (s, 3H, SCH_3), 1.83–2.06 (m, 5H, $\text{CH}_2\text{-CH}_2\text{S}$, pinane-H), 1.42 (s, 9H, $(\text{CH}_3)_3\text{C}$), 1.37 (s, 3H, pinane- CH_3), 1.27 (s, 3H, pinane- CH_3), 1.26 (d, $J = 7.7$ Hz, ^1H , pinane-H), 1.18 (d, $J = 7.5$ Hz, 3H, CH_3CHNH), 0.82 (s, 3H, pinane- CH_3). LC-MS (ESI+) for $\text{C}_{22}\text{H}_{39}\text{BN}_2\text{O}_5\text{S}$ m/z (rel intensity): 477.3 ($(\text{M} + \text{Na})^+$, 23), 455.3 ($(\text{M} + \text{H})^+$, 100), 399.3 ($(\text{M} - \text{CH}_2 = \text{C}(\text{CH}_3)_2 + \text{H})^+$, 23), 355.4 ($(\text{M} - \text{CH}_2 = \text{C}(\text{CH}_3)_2 - \text{CO}_2 + \text{H})^+$, 5), 303.4 ($(\text{M} - \text{pinane} - \text{H}_2\text{O} + \text{H})^+$, 5), 247.3 ($(\text{M} - \text{CH}_2 = \text{C}(\text{CH}_3)_2 - \text{pinane} - \text{H}_2\text{O} + \text{H})^+$, 35), 203.4 ($(\text{M} - \text{CH}_2 = \text{C}(\text{CH}_3)_2 - \text{CO}_2 - \text{pinane} - \text{H}_2\text{O} + \text{H})^+$, 3); $\text{tr} = 18.3$ min; purity >98%. HRMS calcd for $\text{C}_{22}\text{H}_{40}\text{BN}_2\text{O}_5\text{S}$ [$\text{M} + \text{H}$] $^+$, 455.2751; found, 455.2741.

(1R)-1-[*N*-(9-Phenylfluoren-9-yl)-D-methionyl]amino-ethylboronate (+)-Pinanediol Ester (14). Compound (**13**; 0.91 g, 2 mmol)

was dissolved in a 1,4-dioxane solution of HCl (5.0 mL, 4 M) in an ice-cooled bath and stirred for 3 h at room temperature. After being concentrated in vacuo and evaporated three times from chloroform solution, the residue was suspended in anhydrous acetonitrile (10 mL) and sequentially added $\text{Pb}(\text{NO}_3)_2$ (0.66 g, 2.0 mmol), K_3PO_4 (0.85 g, 4.0 mmol), and a solution of PbBr_2 (0.80 g, 2.5 mmol) in CH_3CN (3.0 mL) at room temperature. After being stirred for 48 h, the reaction mixture was filtered through a pad of Celite, and the residue was thoroughly washed with chloroform. The combined filtrates and washings were evaporated and then partitioned between 2.5% aq citric acid (10 mL) and ether (40 mL). The dried organic phase was evaporated to yield the crude product, which was purified by flash column chromatography using EtOAc/hexanes (1/4) to afford **14** (0.94 g, 79% yield) as a white powder. ^1H NMR (CDCl_3) δ 7.62–7.67 (m, 2H, Pf-H), 7.19–7.40 (m, 11H, Pf-H), 6.69 (br d, ^1H , CONH), 4.31 (dd, $J = 8.8$, 2.0 Hz, ^1H , BOCH), 3.97–4.00 (m, ^1H , PfNHCH), 2.90–2.92 (m, ^1H , NH-CHB), 2.85 (br d, ^1H , PfNH), 1.95–2.65 (m, 6H, SCH_2 , pinane-H), 1.93 (s, 3H, SCH_3), 1.65–1.91 (m, 3H, $\text{CH}_2\text{CH}_2\text{S}$, pinane-H), 1.38 (s, 3H, pinane- CH_3), 0.93–1.30 (m, 7H, CH_3CHNH , pinane- CH_3 , pinane-H), 0.85 (s, 3H, pinane- CH_3). LC-MS (ESI+) for $\text{C}_{36}\text{H}_{43}\text{BN}_2\text{O}_3\text{S}$ m/z (rel intensity): 595.5 ($(\text{M} + \text{H})^+$, 42), 461.2 ($(\text{M} - \text{pinane} + \text{H})^+$, 3), 241.2 ($\text{C}_{19}\text{H}_{13}^+$, 100); $\text{tr} = 19.4$ min; purity >95%. HRMS calcd for $\text{C}_{36}\text{H}_{44}\text{BN}_2\text{O}_3\text{S}$ [$\text{M} + \text{H}$] $^+$, 595.3166; found, 595.3179.

(1R)-1-(*S*)-Azetidine-2-carbonyl]amino-ethylboronic Acid (15). L-Azetidine-2-carboxylic acid (0.1 g, 1.0 mmol) was Boc-protected at the N-terminus following the standard procedure.²⁹ The protected product was then coupled to L-boroAla-pn-HCl (270 mg, 1.1 mmol) following the general procedure for the coupling reaction. The protection groups were subsequently removed following the general procedure for pinanediol and Boc removal to give the target as a white powder (0.12 g, 57% yield). ^1H NMR (D_2O) δ 5.10 (t, $J = 8.4$ Hz, ^1H , HNCHCO), 3.98–4.22 (m, 2H, NHCH_2), 3.01 (q, $J = 7.6$ Hz, ^1H , BCHN), 2.76–2.85 (m, ^1H , $\text{NHCH}_2\text{CHACHB}$), 2.59–2.67 (m, ^1H , $\text{NHCH}_2\text{CHACHB}$), 1.18 (d, $J = 7.6$ Hz, 3H, BCHCH $_3$). LC-MS (ESI+) for $\text{C}_6\text{H}_{13}\text{BN}_2\text{O}_3$ m/z (rel intensity): 463.3 ($(3 \times (\text{M} - \text{H}_2\text{O}) + \text{H})^+$, 10), 309.2 ($(2 \times (\text{M} - \text{H}_2\text{O}) + \text{H})^+$, 100), 155.3 ($(\text{M} - \text{H}_2\text{O} + \text{H})^+$, 38); $\text{tr} = 4.9$ min; purity >95%. HRMS calcd for $\text{C}_6\text{H}_{13}\text{BN}_2\text{O}_3\text{Na}$ [$\text{M} + \text{Na}$] $^+$, 195.0917; found, 195.0912.

Acknowledgment. Financial support from Arisaph Pharmaceuticals, Inc. is gratefully acknowledged. One of the authors, G.D.H., was supported by NIH Grant GM067985. We also thank Dr. James Robertson for proofreading the manuscript.

Supporting Information Available: ^1H NMR spectra for the target compounds **1**, **2**, **12**, and **15**; ^{13}C NMR, ^{11}B NMR, and $^1\text{H}/^{13}\text{C}$ HSQC spectra for **1** and **2**; NOESY spectrum for **2**; and CD spectra of compounds **1** and **2** at low and high pH. This material is available free of charge via the Internet at <http://pubs.acs.org>.

References

- De Meester, I.; Korom, S.; Van Damme, J.; Scharpe, S. CD26, let it cut or cut it down. *Immunol. Today* **1999**, *20*, 367–375.
- von Bonin, A.; Huhn, J.; Fleischer, B. Dipeptidyl-peptidase IV/CD26 on T cells: Analysis of an alternative T-cell activation pathway. *Immunol. Rev.* **1998**, *161*, 43–53.
- Hong, W. J.; Doyle, D. Molecular dissection of the NH $_2$ -terminal signal/anchor sequence of rat dipeptidyl peptidase IV. *J. Cell Biol.* **1990**, *111*, 323–328. Iwaki-Egawa, S.; Watanabe, Y.; Kikuya, Y.; Fujimoto, Y. Dipeptidyl peptidase IV from human serum: purification, characterization, and N-terminal amino acid sequence. *J. Biochem.* **1998**, *124*, 428–433. Durinx, C.; Lambeir, A. M.; Bosmans, E.; Falmagne, J. B.; Berghmans, R.; Haemers, A.; Scharpe, S.; De Meester, I. Molecular characterization of dipeptidyl peptidase activity in serum: soluble CD26/dipeptidyl peptidase IV is responsible for the release of X-Pro dipeptides. *Eur. J. Biochem.* **2000**, *267*, 5608–5613.
- Leitung, B.; Pryor, K. D.; Wu, J. K.; Marsilio, F.; Patel, R. A.; Craik, C. S.; Ellman, J. A.; Cummings, R. T.; Thornberry, N. A. Catalytic properties and inhibition of proline-specific dipeptidyl peptidases II, IV and VII. *Biochem. J.* **2003**, *371*, 525–532.

- (5) Meintlein, R. Dipeptidyl-peptidase IV (CD 26): Role in the inactivation of regulatory peptides. *Regul. Pept.* **1999**, *85*, 9–24.
- (6) Deacon, C. F. Therapeutic strategies based on glucagon-like peptide 1. *Diabetes* **2004**, *53*, 2181–2189.
- (7) Drucker, D. J. Therapeutic potential of dipeptidyl peptidase IV inhibitors for the treatment of type 2 diabetes. *Expert Opin. Invest. Drugs* **2003**, *12*, 87–100. Augustyns, K.; Van der Veken, P.; Senten, K.; Haemers, A. Dipeptidyl peptidase IV inhibitors as new therapeutic agents for the treatment of type 2 diabetes. *Expert Opin. Ther. Pat.* **2003**, *13*, 499–510.
- (8) Flentke, G. R.; Munoz, E.; Huber, B. T.; Plaut, A. G.; Kettner, C. A.; Bachovchin, W. W. Inhibition of dipeptidyl aminopeptidase IV (DP-IV) by Xaa-boroPro dipeptides and use of these inhibitors to examine the role of DP-IV in T-cell function. *Proc. Natl. Acad. Sci. U.S.A.* **1991**, *88*, 1556–1559.
- (9) Gutheil, W. G.; Bachovchin, W. W. Separation of L-Pro-DL-boroPro and its component diastereomers and kinetic analysis of their inhibition of dipeptidyl peptidase IV. A new method for the analysis of slow, tight-binding inhibition. *Biochemistry* **1993**, *32*, 8723–8931.
- (10) Snow, R. J.; Bachovchin, W. W. Boronic acid inhibitors of dipeptidyl peptidase IV: A new class of immunosuppressive agents. *Adv. Med. Chem.* **1995**, *3*, 149–177.
- (11) Sudmeier, J. L.; Gunther, U. L.; Gutheil, W. G.; Coutts, S. J.; Snow, R. J.; Barton, R. W.; Bachovchin, W. W. Solution structures of active and inactive forms of the DPP IV (CD26) inhibitor Pro-boroPro determined by NMR spectroscopy. *Biochemistry* **1994**, *33*, 12427–12438.
- (12) Snow, R. J.; Bachovchin, W. W.; Barton, R. W.; Cambell, S. J.; Coutts, S. J.; Freeman, D. M.; Gutheil, W. G.; Kelly, T. A.; Kennedy, C. A.; Krolkowski, D. A.; Leonard, S. F.; Pargellis, C. A.; Tong, L.; Adams, J. Studies on proline boronic acid dipeptide inhibitors of dipeptidyl peptidase IV: Identification of a cyclic species containing a B–N bond. *J. Am. Chem. Soc.* **1994**, *116*, 10860–10869.
- (13) Coutts, S. J.; Kelly, T. A.; Snow, R. J.; Kennedy, C. A.; Barton, R. W.; Adams, J.; Krolkowski, D. A.; Freeman, D. M.; Campbell, S. J.; Ksiazek, J. F.; Bachovchin, W. W. Structure-activity relationships of boronic acid inhibitors of dipeptidyl peptidase IV. 1. Variation of the P2 position of Xaa-boroPro dipeptides. *J. Med. Chem.* **1996**, *39*, 2087–2094.
- (14) Heins, J.; Welker, P.; Schoenlein, C.; Born, I.; Hartrodt, B.; Neubert, K.; Tsuru, D.; Barth, A. Mechanism of proline-specific proteinases: (I) Substrate specificity of dipeptidyl peptidase IV from pig kidney and proline-specific endopeptidase from *Flavobacterium meningosepticum*. *Biochim. Biophys. Acta.* **1988**, *954*, 161–169.
- (15) Hu, Y.; Ma, L.; Wu, M.; Wong, M. S.; Li, B.; Corral, S.; Yu, Z.; Nomanbhoy, T.; Alemayehu, S.; Fuller, S. R.; Rosenblum, J. S.; Rozenkrants, N.; Minimo, L. C.; Ripka, W. C.; Szardenings, A. K.; Kozarich, J. W.; Shreder, K. R. Synthesis and structure–activity relationship of N-alkyl Gly-boro-Pro inhibitors of DPP4, FAP, and DPP7. *Bioorg. Med. Chem. Lett.* **2005**, *15*, 4239–4242.
- (16) Freidinger, R. M.; Perlow, D. S.; Veber, D. F. Protected lactam-bridged dipeptides for use as conformational constraints in peptides. *J. Org. Chem.* **1982**, *47*, 104–109. Freidinger, R. M. Design and synthesis of novel bioactive peptides and peptidomimetics. *J. Med. Chem.* **2003**, *46*, 5553–5566.
- (17) Cahn, R. S.; Ingold, C.; Prelog, V. Specification of molecular chirality. *Angew. Chem., Int. Ed. Engl.* **1966**, *5*, 385–415.
- (18) Pechenov, A.; Stefanova, M. E.; Nicholas, R. A.; Peddi, S.; Gutheil, W. G. Potential transition state analogue inhibitors for the penicillin-binding proteins. *Biochemistry* **2003**, *42*, 579–588.
- (19) Kienhofer, A. 1-Hydroxy-7-azabenzotriazole (HOAt) and N-[(dimethylamino)-1H-1,2,3-triazolo-[4,5-b]pyridin-1-yl-methylene]-N-methylmethanaminium hexafluorophosphate N-oxide (HATU). *Synlett* **2001**, *11*, 1811–1812.
- (20) Thaisrivongs, S.; Pals, D. T.; Turner, S. R.; Kroll, L. T. Conformationally constrained renin inhibitory peptides: γ -Lactam-bridged dipeptide isostere as conformational restriction. *J. Med. Chem.* **1988**, *31*, 1369–1376.
- (21) Matteson, D. S.; Lu, J. Asymmetric synthesis of 1-acyl-3,4-disubstituted pyrrolidine-2-boronic acid derivatives. *Tetrahedron: Asymmetry* **1998**, *9*, 2423–2436.
- (22) Lubell, W. D.; Rapoport, H. Configurational stability of N-protected α -amino aldehydes. *J. Am. Chem. Soc.* **1987**, *109*, 236–239.
- (23) Feldman, P. L.; Rapoport, H. Synthesis of optically pure Δ^4 -tetrahydroquinolinic acids and hexahydroindolo[2,3-a]quinolizines from L-aspartic acid. Racemization on the route to vindoline. *J. Org. Chem.* **1986**, *51*, 3882–3890.
- (24) Bernstein, F. C.; Koetzle, T. F.; Williams, G. J. B.; Meyer, E. F.; Brice, M. D.; Kennard, O.; Shimanouchi, T.; Tasumi, M. The Protein Data Bank: A computer-based archival file for macromolecular structures. *J. Mol. Biol.* **1977**, *112*, 535.
- (25) Hiramatsu, H.; Yamamoto, A.; Kyono, K.; Higashiyama, Y.; Fukushima, C.; Shima, H.; Sugiyama, S.; Inaka, K.; Shimizu, R. The crystal structure of human dipeptidyl peptidase IV (DPPIV) complex with diprotin A. *Biol. Chem.* **2004**, *385*, 561–564.
- (26) Engel, M.; Hoffmann, T.; Manhart, S.; Heiser, U.; Chambre, S.; Huber, R.; Demuth, H. U.; Bode, W. Rigidity and flexibility of dipeptidyl peptidase IV: Crystal structures of and docking experiments with DPPIV. *J. Mol. Biol.* **2006**, *355*, 768–783.
- (27) Khan, A. R.; Parrish, J. C.; Fraser, M. E.; Smith, W. W.; Bartlett, P. A.; James, M. N. G. Lowering the entropic barrier for binding conformationally flexible inhibitors to enzymes. *Biochemistry* **1998**, *37*, 16839–16845.
- (28) (a) Püschel, G.; Meintlein, R.; Heymann, E. Isolation and characterization of dipeptidyl peptidase IV from human placenta. *Eur. J. Biochem.* **1982**, *126*, 359–365. (b) Heins, J.; Welker, P.; Schönlein, C.; Born, I.; Hartrodt, B.; Neubert, K.; Tsuru, D.; Barth, A. Mechanism of proline-specific proteinases: (I) Substrate specificity of dipeptidyl peptidase IV from pig kidney and proline-specific endopeptidase from *Flavobacterium meningosepticum*. *Biochim. Biophys. Acta* **1988**, *954*, 161–169. (c) Rahfeld, J.; Schutkowski, M.; Faust, J.; Neubert, K.; Barth, A.; Heins, J. Extended investigation of the substrate specificity of dipeptidyl peptidase IV from pig kidney. *Biol. Chem. Hoppe–Seyler* **1991**, *372*, 313–318.
- (29) Guanti, G.; Riva, R. Synthesis of chiral non-racemic azetidines by lipase-catalyzed acetylations and their transformation into amino alcohols: precursors of chiral catalysts. *Tetrahedron: Asymmetry* **2001**, *12*, 605–618.

JM061321+